Malaria β-Haematin in blood results in synergistic attenuation enhancement: Studies with a conventional multimode reader and a custom LED device

Eugene Y. Chan[1]*, Kristyn Maiorca[1], Candice Bae[1], Nathaniel Sharpe[1], Vinay Tripuraneni[2], Julia Z. Sharpe[1]

[1]DNA Medicine Institute, 727 Massachusetts Avenue, Cambridge, MA 02139-3323, USA

[2]Duke University School of Medicine, Durham, NC 27710, UK

*echan@dnamedinstitute.com

1 Introduction

Malaria is a global disease, affecting tropical and subtropical regions of Africa, Asia, and South and Central America. It is transmitted through the bite of the *Anopheles* mosquito. Infected individuals have an acute fever, chills, headache, and vomiting. The following are some stark statistics about the disease: (1) close to a quarter billion individuals suffer from the disease at any given time, (2) an estimated 781,000 individuals died from the disease in 2009, (3) a child in Africa dies of the disease every 45 seconds, and (4) 20% of all childhood deaths in Africa are caused by the disease [1].

To date there are limited methods for diagnosis of the disease. The gold standard for malaria diagnosis is microscopy of Giemsa-stained blood smears. This approach involves blood collection, slide preparation, and manual counting of infected cells. Routine detection limits for microscopy are approximately 50-100 parasites/μL [2,3]. Even with well-trained microscopists, false positives and negatives can occur, leading to variability in diagnosis. The requirements for training and equipment limit the applicability of this technique to reasonably resourced medical settings.

Molecular methods are suitable alternatives to microscopy. These include the rapid diagnostic tests (RDTs) for malaria, which are based on the immunochromatographic assay [4]. RDTs are based on the use of monoclonal antibodies directed against malaria antigen. RDTs are by nature qualitative, require some manual sample handling, and require a cold chain for transport. Other methods for malaria detection include the polymerase chain reaction [5], fluorescence thin blood smears [6], and flow cytometry [7,8]. Unlike the RDTs, these other methods all require specialised and costly equipment. At present, all these approaches still require blood draws, which carry the risk of blood-borne pathogen transmission.

The development of a malaria diagnostic test based on malarial hemozoin (HZ) can take advantage of its biophysical properties. Hemozoin is formed from the heme groups released by the *Plasmodium* parasite upon digestion of hemoglobin. β-haematin (BH) is the chemically synthesised form of malarial hemozoin. It is identical to malarial hemozoin, chemically, structurally, and spectroscopically [9,10]. Both have the chemical composition of $(Fe^{III}$-protoporphyrin-IX$)_2$, have identical X-ray diffraction patterns [11], and have identical crystal structures [12]. Due to the oxidation of iron from Fe^{2+} to Fe^{3+}, hemozoin possesses paramagnetic properties. Furthermore, both have identical Fourier transform infrared [10] and absorbance spectra [13,14]. Their identical characteristics make them interchangeable for studies.

Malarial hemozoin's crystal properties have been studied. In particular, the crystal is birefringent [15]. When light passes through the crystal, it is doubly refracted, resulting in two rays. This property can be utilised to diagnose malaria via polarised light microscopy. Infected red blood cells with hemozoin have unique scattering profiles [16], which can be measured with dark-field microscopy in conjunction with cross-polarisation imaging. Hemozoin and infected red blood cells have unique light scattering properties [17,18]. Elastic and backscattered light have unique profiles for the infected cells. Refractive index maps of infected red blood cells results in unique profiles, in part due to the presence of hemozoin [19]. Light scattering and polarisation studies, however, have been focused on thin smears of blood cells. The optical properties of hemozoin in bulk solutions are less well studied.

Bulk solution studies are important because they are done on size scales required for non-invasive detection, such as across a finger or earlobe. Most notably, this includes monitoring the magnetically-induced dichroism of malaria hemozoin using polarised light [20,21]. This approach utilises the Cotton-Mouton effect upon application of an applied magnetic field and the orthogonal polarised light for detection. This method has been utilised successfully with BH and HZ in solution and also blood samples with lysed cells, but not on bulk, turbid solutions with intact cells [22]. For these polarisation-based approaches,

https://doi.org/10.5281/zenodo.10894792

the challenge is accounting for rapid depolarisation of light as it is transmitted through tissue and blood samples.

2 The idea

The idea behind our GCE grant (Round 4, 2010) was to develop a non-invasive method for diagnosing malaria. In order to do this, we sought to identify a novel optical property of β-haematin that gives it a robust optical signature. The optical signature needs to be readily detected with light-emitting diodes (LEDs) and photodiodes, which are compatible with low-cost operation in the developing world. The product is envisioned to be similar to a commercial fingertip pulse oximeter, which can be purchased for $20 and can be utilised for thousands of tests with a single battery.

We hypothesised that measurement of light attenuation is a potential approach to detect malarial hemozoin. For instance, light attenuation is utilised by conventional pulse oximeters to measure heart rate and oxygen saturation. Calculations based on the Beer-Lambert law suggest that only high levels of hemozoin, greater than 5 μg/mL, are detectable. These calculations, however, utilise the assumption of non-turbid media. Light attenuation has dramatically different traits in blood, a turbid and highly scattering media. It is conceivable that hemozoin in blood would have unexpected attenuation traits. In this grant, we sought to investigate the effects of BH in blood on light attenuation. The presence of unique light signatures, especially detectable through light attenuation would allow for the development of a simple LED-based method of malarial hemozoin detection, which can potentially be used as the basis for non-invasive diagnosis, through finger detection.

3 Results

Here, using β-haematin, a chemically and spectroscopically identical form of hemozoin, we demonstrate that β-haematin in blood leads to larger than predicted light attenuation enhancement when compared to attenuation values for blood or β-haematin alone. We discovered greater than expected light attenuation when low concentrations of β-haematin are mixed with blood. The attenuation is much greater than the sum of the attenuations for BH and blood. We term this phenomenon, "synergistic attenuation enhancement" (SAE), which allows for ultrasensitive detection of BH in human blood. This synergistic attenuation enhancement is significant and measurable down to 6 pg/mL of β-haematin, a concentration equivalent to a few *Plasmodium*-infected erythrocytes per μL. This lower limit of detection is 10^6 better than what may be suggested by the Beer-Lambert law. Wavelength dependence is observed, with the SAE effect greater at shorter wavelengths. The effect is observed with both a conventional spectrophotometer as well as a custom photodiode device that utilizes an LED and two photodiodes. With both methods, we demonstrate the SAE effect is present and significant for detection of BH at levels required for malaria diagnosis. The data shows that ultrasensitive bulk detection of β-haematin in blood is possible.

3.1 Synergistic attenuation enhancement

Conventionally, absorbance of light through a non-scattering media is the sum of its constituent parts according to the Beer-Lambert law, which states that the total absorbance of the media is the sum of the individual absorbances. It is also well known that blood and other particulates have non-linear effects due to the effects of multiple scattering centres based on their respective size and refractive indices [22,23]. Thus for particulates, the total attenuation is from the sum of its absorbance and scattering contributions. For blood it has been shown that optical densities (ODs) for non-hemolysed blood are much different than hemolysed blood at certain wavelengths [23,24]. It is possible, therefore, that introduction of another particulate into a blood suspension can lead to changes in multiple scattering and measurable differences in OD. We performed a series of experiments to assess the SAE effect by spiking-in BH into blood.

In the first experiment, we characterised the light attenuation of BH and blood. To characterise the light attenuation of a BH and blood mixture, we measured the attenuation of a 4% hematocrit (Hct) blood sample and a titration of BH separately and subsequently as a mixture. For the 4 mm path length cuvette, this hematocrit was utilised so that measurements could be taken without saturating the OD reading of the spectrophotometer. In later experiments, we worked with whole blood and other blood concentrations. For this experiment, a frosted glass cuvette was utilised to diffuse light similar to various finger models developed for pulse oximetry [25]. Clear cuvettes gave similar results except that the frosted cuvettes increase the baseline scattering of the system and do not change the observed signal changes. The experiments were performed with a commercial spectrophometer using a 645 nm wavelength. The expected value, based on summation of the attenuations, is from the BH titration in 1x phosphate buffered saline (1x PBS) and the test blood sample. The expected versus the actual attenuation is shown in Fig. 1A. The corresponding percentage light transmission %T is plotted in Fig. 1B. The measurements for the expected attenuation are the sum of the blank blood samples and the BH titration in 1x PBS. The attenuation for the expected is only measurable at greater than ~5 μg/mL of BH. In contrast, when BH is spiked into blood, there is a significant attenuation enhancement. The lowest concentration tested, 6.7 pg/mL BH in blood was detectable with a p-value < 0.005 (Fig. 1C).

We performed visible wavelength attenuation spectral measurements on BH in 1x PBS and also in blood. The measurements for BH in 1x PBS are shown in Fig. 1D.

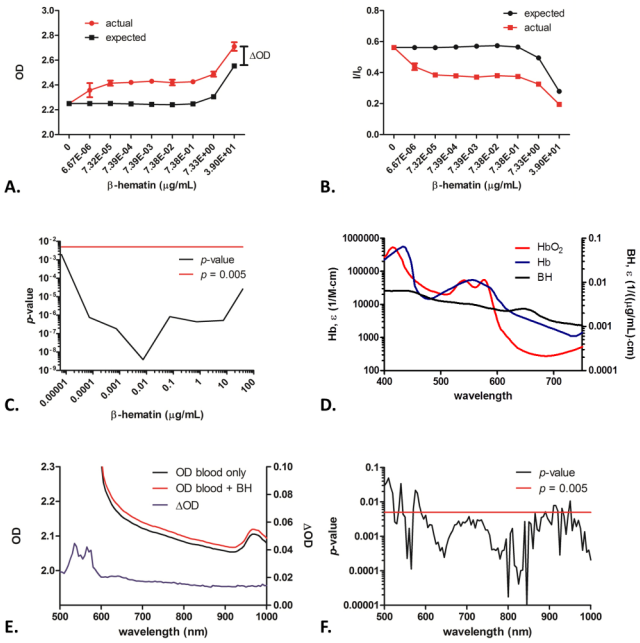

Figure 1. Synergistic attenuation enhancement of β-haematin in blood, measured with a conventional spectrophotometer. (A) Attenuation (OD) at 645 nm versus β-haematin concentration measured with a SpectraMax M2. β-haematin spiked into blood gives rise to enhanced attenuation. Error bars ± SEM, N = 3. The red line is the actual signal whereas the black line is the expected signal based on the extinction coefficient of BH. (B) Light transmission versus β-haematin concentration. (C) *p*-value of differences between samples for OD versus [BH] graph. (D) Absorbance spectra of oxygenated hemoglobin (HbO_2), deoxygenated hemoglobin (Hb) overlayed with β-haematin spectra. The BH extinction coefficient (ε) is expressed with the concentration term in μg/mL. HbO_2 and Hb spectra from http://omlc.ogi.edu/. (E) OD and ΔOD versus wavelength of 0.67 μg/mL β-haematin in blood. Error bars ± SEM, N = 3. The black line is the spectra prior to spike-in, the red line after spike-in with BH, and the blue line the difference between the two spectra. (F) *p*-value versus λ of unpaired two-tailed *t*-tests between spectra.

The measurements show that BH has a small attenuation peak at approximately 640 nm, consistent with previous findings in the literature [26]. Other than this small peak there are no significant distinguishing peaks. The spectrum is shown with those from oxygenated and deoxygenated hemoglobin. This peak is a unique feature for BH when compared with spectra for hemoglobin. Based on its extinction coefficient this peak should be detectable at greater than ~5 μg/mL of BH. The equivalent percentage parasitemia may be estimated from the BH concentration and depends on the parasite stage, tissue distribution, and free hemozoin. Concentrations of BH at the μg/mL level most likely correspond to the higher range of clinically observed parasitemia levels (see Discussion). To assess the spectral features of a spiked blood sample, we performed spectral measurements of blood alone and blood with 670 ng/mL BH (Fig. 1E). Without the SAE effect, we would expect that at the measured concentration the difference between the spiked blood sample and the original blood sample would yield almost no difference at all the wavelengths measured. Instead, we observed that the entire spectra shifted up with the spiked sample. The ΔOD trace, which measures the difference between the two spectra, shows attenuation enhancement across wavelengths from 500 nm to 1000 nm. The ΔOD varies with wavelength. For instance, at 545 nm, ΔOD is 0.035 and at 645 nm, it is 0.021. The magnitude of the measured ΔOD was lower than those in Fig. 1A-C, which was likely due to the lower blood concentration (1% hematocrit) used to keep the spectrophotometer within range for the full spectra. The spectral results show that the SAE effect is greatest at blood's most strongly absorbing regions. There are two distinct peaks between 500 and 600 nm, which are similar to those found in HbO_2. A small hump is seen at 630-640 nm, which could be related to the BH peak. An increased effective path length for light traveling through the blood/BH mixture, such as in multiple scattering, can potentially account for this observation. The *p*-value, as determined by an unpaired two-tailed *t*-test, between the two spectra is plotted versus the wavelength (Fig. 1F). The majority of the differences have *p*-values < 0.005, indicating high statistical likelihood for a real difference between the spectra with and without BH. The *p*-value for 545 and 645 nm, two wavelengths utilised in our custom LED device, described later, are 0.0044 and 0.00024, respectively.

3.2 Multiple wavelength spike-in experiments

Spike-in time course experiments were performed with multiple wavelengths for 1% and 50% hematocrits. The 50% hematocrit was whole human blood. Based on the spectral data, the SAE effect should be greater in the green region than the red or infrared regions. The raw data from each of the wavelengths for the 1% Hct experiments exhibit the SAE effect shortly after BH spike-in (Fig. 2A). Multiple data points were taken prior to the spike-in as a baseline. Ratios of the wavelengths for 545 nm to the other tested wavelengths exhibited an increase after the spike-in (Fig. 2B). This indicates that the SAE effect is greater at 545 nm than the other red and infrared wavelengths. The red to infrared ratios do not exhibit this increase (Fig. 2C). These multiple wavelength time course experiments allow us to verify the signal repeatability prior to the BH spike-in. This allows verification that the blood samples are

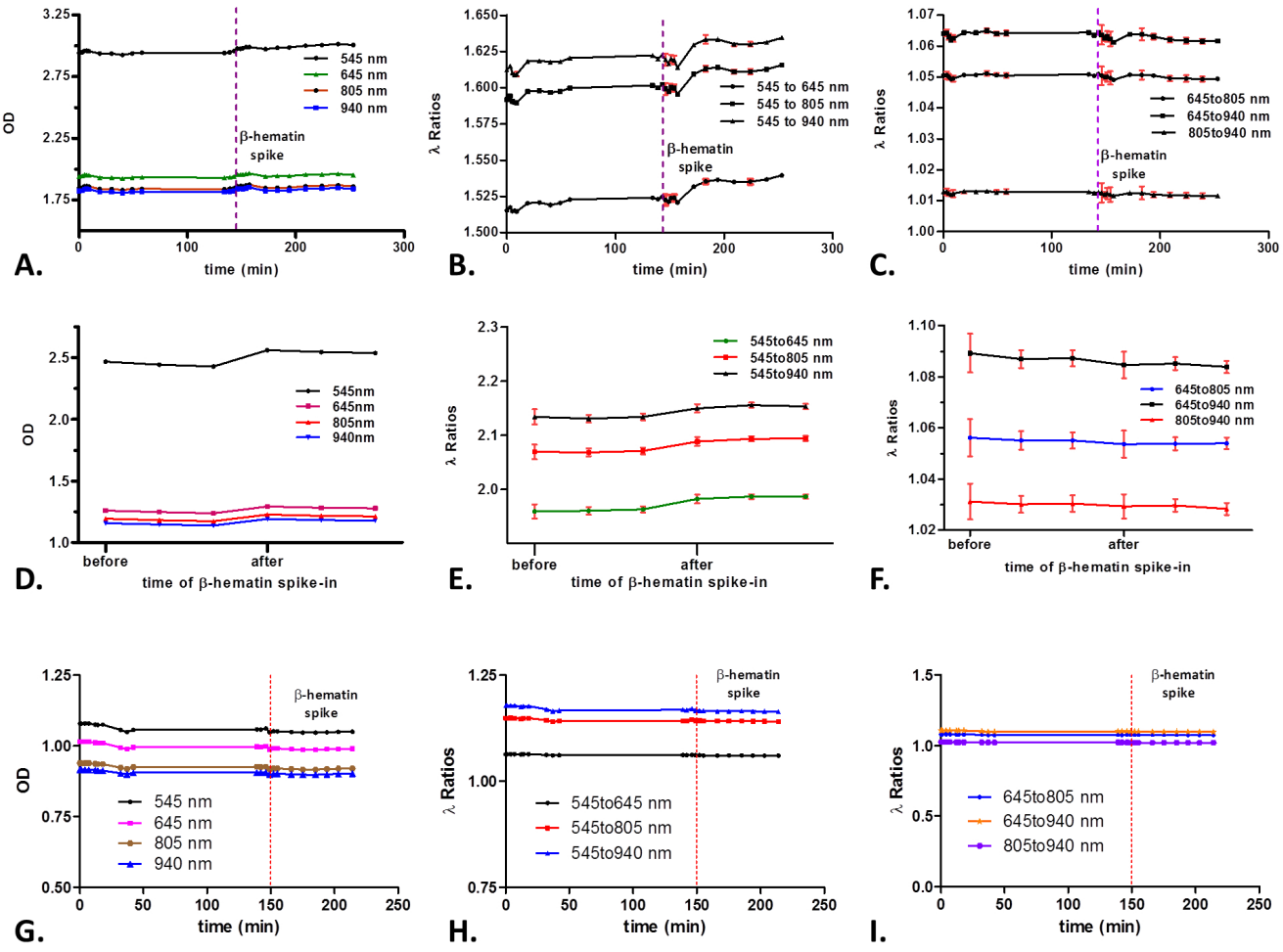

Figure 2. Time course spike-in experiments with β-haematin. (A) BH spiked-in to a final concentration of 0.67 µg/mL in 1% hematocrit. The time of spike-in is indicated on the graph by the vertical dashed line. Four different wavelengths are recorded versus time: 545, 645, 805, and 940 nm. (B) Ratiometric wavelength analysis of the BH spike-in time course experiment in (A). The wavelength λ ratios are shown for 545:645 nm, 545:805 nm, and 545:940 nm. (C) Ratiometric wavelength analysis of the time course experiment in (A) for ratios of 645:805 nm, 645:940 nm, and 805:940 nm. (D) BH spiked-in to a final concentration of 0.67 µg/mL in whole human blood at 50% hematocrit. Data points taken at 5 min intervals and are shown for four wavelengths before and after spike-in. (E) Ratiometric wavelength analysis of the time course experiment in (D) for ratios 545:645 nm, 545:805 nm, and 545:940 nm. (F) Ratiometric wavelength analysis of the time course experiment in (D) for ratios 645:805 nm, 645:940 nm, and 805:940 nm. (G) Negative control spike-in experiments of BH into 1x phosphate buffered saline (1x PBS) to a final BH concentration of 0.67 µg/mL. (H) Ratiometric wavelength analysis of the time course experiment in (G) for ratios of 545:645 nm, 545:805 nm, and 545:940 nm. (I) Ratiometric wavelength analysis of the time course experiment in (G) for ratios of 645:805 nm, 645:940 nm, and 805:940 nm. All error bars ± SEM, N = 3.

equilibrated with room air and are not deoxygenating over time. The experiments were repeated with whole human blood at 50% hematocrit in a clear 0.25 mm path length cuvette. The shorter path length was required in order to remain within range on the spectrophotometer. The SAE effect was observed for the whole blood experiments as well. The raw data highlights the increase in signal upon spike-in of the BH (Fig. 2D). The ratios of 545 nm to the longer wavelengths exhibited an increase (Fig. 2E), whereas the longer wavelength ratios were constant (Fig. 2F). The multiple wavelength assessment is consistent with the spectral characteristics of the SAE effect. The overall magnitude of the λ ratios, before and after spike-in, is greater for 50% hematocrit than 1% hematocrit. This could be due to the increase in scattering centres. Negative control experiments were performed by spiking in BH into 1x PBS instead of blood. The results of the time course are shown in Fig. 2G. No observable differences in the measured OD

were present before and after the spike-in. None of the λ ratios yielded any observable differences (Fig. 2H-I). These experiments highlight the differences when BH is spiked into saline versus blood.

3.3 90° light scattering studies

Previous work in the field has shown that infected red blood cells and hemozoin have unique light scattering properties [17,18,27,28]. In contrast with these studies, which performed examinations on thin smear samples, typically under a microscope coverslip, our light scattering studies were performed on bulk, in cuvette solutions. We examined light scattering at 90° to assess whether the increase in OD is from increased scattered light. An increase in light scattering would lead to an observed decrease in attenuation. In our experiments, the incident beam was directed to a frosted side of the cuvette with a 4 mm path length and collected at 90° through a clear window. Data was collected with 4% hematocrit blood and spiked with BH to a final concentration of 670 ng/mL. A decrease in scattered light is observed for 545 and 570 nm (Fig. 3A). The light scattering does not change significantly before and after spike-in for 645 nm and 805 nm (Fig. 3B). Similar to the attenuation measurements, the shorter wavelengths resulted in a greater change of signal than 645 or 805 nm. The results are analysed using a grouped analysis, as shown in Fig. 3C-D for the various wavelengths assessed. The values before the spike-in and after spike-in are represented and their *p*-values calculated to determine the presence of significant differences between the groups using an unpaired *t*-test. For both the 545 and 570 nm wavelengths there is a statistically significant difference before and after BH spike-in ($p < 0.0001$). In contrast, the longer wavelengths, 645 and 805 nm do not have statistically significant changes ($p=0.1704$, $p=0.1829$ respectively). A similar type of group analysis was performed to examine the various λ ratios, which is shown in Fig. 3E-F. The ratios 545:645 nm, 570:645 nm, and 570:805 nm resulted in statistically significant differences ($p=0.0003$), whereas the ratios 645:805 nm, 545:805 nm, and 545:570 nm resulted in no significant differences. Unlike the attenuation measurements, the 545:805 nm ratio did not result in a significant change. This could be because light scattering is a less sensitive method of measuring the SAE effect. Overall, these results, like the attenuation measurements, show wavelength dependence, with the 545 and 570 nm wavelengths exhibiting a greater change in signal upon spike-in. The measured decrease in light scattering gives further insight into the mechanism of the SAE effect. For 0° and 90°, a greater amount of light is absorbed, which could result from multiple scattering, resulting in a longer effective path length required for light to travel through the sample. Furthermore, it is differentiated from resonance light scattering [29,30], which gives rise to measurable increased 90° light scattering based on electronically coupled chromophore arrays.

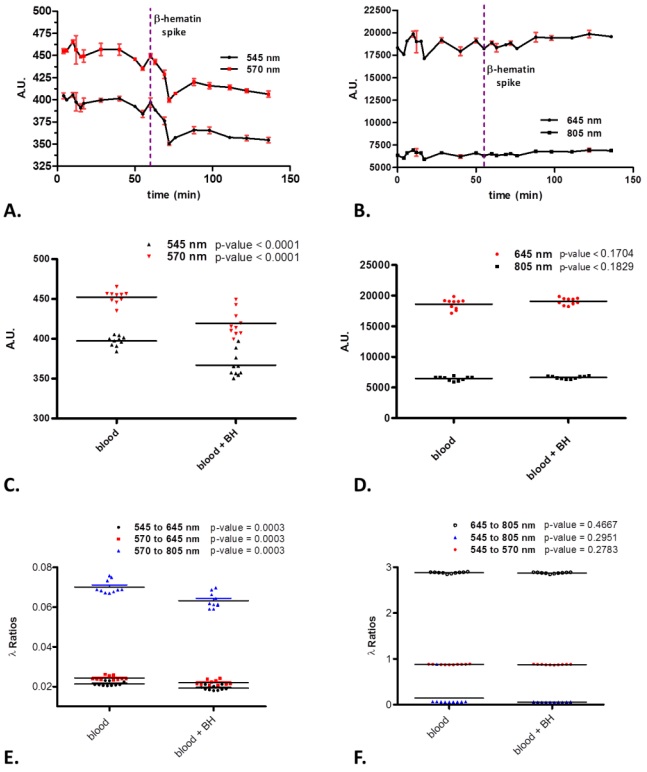

Figure 3. β-haematin spike-in 90° light scattering experiment. (A) Time course of 90° light scattering measurements of BH spiked into blood at 1% hematocrit. The final BH concentration is 0.67 µg/mL. The vertical dashed line represents the time of BH spike-in. The vertical axis represents arbitrary units (A.U.), or the amount of scattered light as measured by the photomultiplier tube on the SpectraMax M2. (B) 645 and 805 nm time course of 90° light scattering measurements of BH spiked into blood. Measurements performed concurrently with those shown in (A). (C) Grouped plots of the data points before and after the spike-in for the light scattering experiments. 545 and 570 nm are shown. The *p*-value is calculated for each wavelength data set before and after spike-in using an unpaired *t*-test. (D) Grouped plots for 645 and 805 nm before and after spike-in for the light scattering experiments. (E) Grouped ratiometric wavelength analysis of the experiment. The wavelength ratio 545:645 nm, 570:645 nm, and 570:805 nm are compared before and after the spike-in. The *p*--values comparing before and after the spike-in are shown. (F) Grouped ratiometric wavelength analysis for the ratios 645:805 nm, 545:805 nm, and 545:570 nm. The *p*--values comparing before and after the spike-in are shown.

3.4 Design of custom LED scanner for measurements

Based on the SAE measurements, ratiometric measurements of a green wavelength to a red or infrared wavelength allow detection of BH in blood. We selected two wavelength ranges for assessing the SAE effect, 540-550 nm and 640-650 nm. Any one of the other wavelength pairs that gave a significant change could have been selected. 545 nm is one of the isosbestic points of hemoglobin and thus allows a suitable reference regardless of hemoglobin oxygenation. 805 nm is another isosbestic point that could be utilised, allowing for a ratio of two isosbestic points as the measurement method. In our tests, since oxygenation was not varied, we could utilise any one of the three wavelengths tested (645, 805, and 940 nm). We selected 645 nm as the second wavelength since this allowed us to use a single white LED as the illumination source. Based on our results using conventional spectrophotometry, we reasoned that by electronically amplifying the light transmission ratio between 540-550 nm and 640-650 nm, the device could readily detect the presence of trace amounts of BH in human blood due to the SAE effect.

3.5 LED scanner overview

We built a custom handheld reader for measuring light transmission at two wavelengths. Figure 4A-B shows the experimental apparatus utilised for the measurements. The apparatus has a blackened cuvette insertion slot, batteries, electronics, light-emitted diode (LED), photodiodes, filters, and data acquisition card. The device utilises a single Ce^{3+}:YAG phosphor-based white LED for illumination. This broadband source has a primary emission peak at 405 nm and a spectrum that goes to 750 nm. Colour filters for green and red are placed in front of the photodiodes. The output from the photodiodes is amplified via a two-stage op amp circuit (Fig. 4C). Each stage is based on a low drift, low power instrumentation amplifier. The total amplification between the two photodiodes is the product of the gain from each stage and can be adjusted independently.

3.6 β-Haematin detection using LED scanner

Cuvettes containing β-haematin and blood or with blood alone were inserted into the reader and the voltage reading from the two-stage amplifier obtained. Blackened cuvettes with 1 cm path lengths and clear windows were utilised for the experiment. 4% Hematocrit was utilised, a 1 in 10 dilution of whole blood, in 1x PBS. The dilution was required to allow light to pass through to the photodiodes. This concentration is similar to the amount of blood contained in human tissue, in which blood is 8% of the tissue volume. A hematocrit of 50% would mean that 4% of the volume is occupied with blood cells. At 4% hematocrit this allowed us to approximate the light levels as would be through a 1 cm path length of human tissue. Figure 4D shows the raw data from experiments at 500 ng/mL BH. The raw data shows exchange of a normal sample with a spiked sample in two different cuvettes. The results show blood and β-haematin samples having different voltage readings. During the cuvette change large voltage changes are observed since one photodiode is transiently blocked while the other is fully exposed to the light. Upon insertion of the cuvette the voltage reading correctly identifies the sample. We estimated the minimum readout time to be 1-2 seconds.

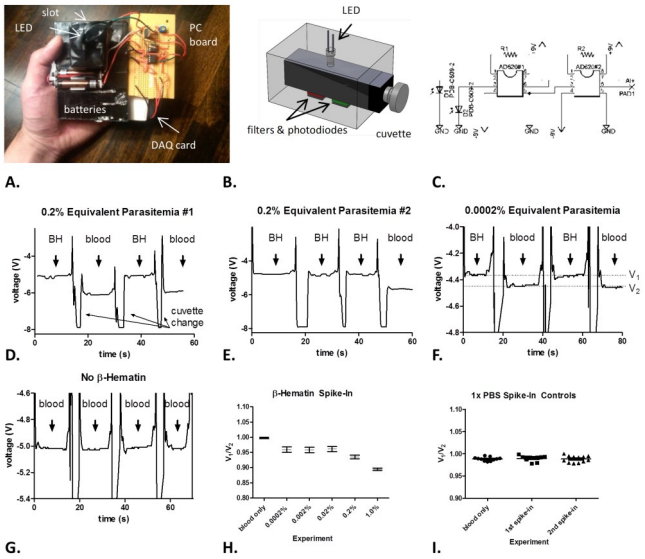

Figure 4. β-haematin spike-in experiments performed in a custom-built LED device. (A) Photograph of the device with LED, cuvette slot, batteries, PC board, and DAQ card. (B) Detailed image of the OFS body comprising cuvette, cuvette holder, green filter, red filter, photodiodes, and white LED. (C) Electrical circuit diagram of the two-stage difference amplifier. R1 = 1kΩ, R2 = 100Ω or 147Ω. (D) Detection of β-haematin in human blood at 0.2% equivalent parasitemia levels. Calculation of equivalent parasitemia level described in text. Voltage versus time data trace with alternating blood and β-haematin cuvettes. The β-haematin reads at a more positive voltage. (E) Data trace for a different sequence of cuvette loads showing detection of β-haematin at 0.2% equivalent parasitemia levels. Experiments performed with gain = 17k. (F) β-haematin spike-in at 0.0002% equivalent parasitemia. (G) Negative control with blood only in both cuvettes. (H) Spike-in experiment of β-haematin shows statistically significant detection ($p < 0.0001$) from 0.0002% (0.0005 µg/mL) to 1.0% (2.5 µg/mL) equivalent parasitemia levels. Error bars ± SEM (N = 12-17). Experiments performed with gain = 17k. (I) 1x PBS spike-in control experiment with 1x PBS only into blood. No statistically significant differences in the spike-ins and blood only ($p = 0.5562$ and $p = 0.9851$ for first and second spike-in, respectively). Experiments performed with gain = 25k.

The loading sequence was varied in different cases, which had no effect on the correct identification of the β-haematin sample (Fig. 4E). The equivalent parasitemia level was calculated based on an estimation of 0.3 pg hemozoin (HZ) per infected RBC [31-33]. The amount of hemozoin depends on the parasite stage but we utilised this number as the average. For $4.2x10^6$ cells per µL, 0.4% equivalent parasitemia corresponds to 5.0 µg HZ per mL. Since we utilised 10-fold diluted whole human blood, we utilised a β-haematin cuvette concentration of 0.5 µg/mL to maintain the same relative concentration of β-haematin in red blood cells. A 1000-fold lower concentration sample was tested under the same experimental conditions (Fig. 4F). Clear changes are observed between the 500 pg/mL BH sample and the control blood sample. With a 0.3 pg HZ/cell, this corresponds to a 0.0004% estimated parasitemia level. Controls with blood only in both cuvettes were performed, showing equivalent signal levels for both cuvettes (Fig. 4G).

3.7 Spike-in titration for LED scanner

The device's detection capabilities were further examined by spike-in titration experiments. A human blood sample was split equally between two identical blackened cuvettes with clear windows. These cuvettes were tested against each other to rule out any differences in cuvettes and cuvette insertion. Increasing amounts of β-haematin were added to one of the cuvettes and the difference measured between that and blood only sample. Various sample concentrations, spanning 500 pg/mL (estimated to be 0.0004% parasitemia at 0.3 pg HZ/infected cell) to 2.5 µg/mL (estimated to be 2.0% parasitemia at 0.3 pg HZ/infected cell) were assessed. The ratio of the first cuvette's voltage V_1 to the second cuvette's voltage V_2 was utilised as a normalised measure of the signal to correct for any voltage drift. The results from the test are shown in Fig. 4H. All tested concentrations of β-haematin were detected with statistical significance of $p< 0.0001$ using an unpaired two-tailed t-test. The V_1/V_2 ratio was equivalent for 0.0004%, 0.004%, and 0.04%. The ratio followed a linear trend for the higher concentrations. Negative spike-in controls with 1x PBS only were assessed. These controls were performed to rule out any differences from the addition of 1x PBS and also to exclude the possibility that mixing of the sample would lead to any detectable differences between the two samples (Fig. 4I). From the 1x PBS spike-in controls, no statistically significant (p=0.5562, 0.9851) differences between the spike-ins and the blood only samples.

4 Discussion

Based on the above results we developed a model for synergistic attenuation enhancement. β-Haematin in blood gives rise to an unexpected synergistic attenuation enhancement ΔOD when compared to attenuation values for blood or β-haematin alone. Conventionally, absorbance of light through a medium is the sum of its constituent parts. In our measurements, we observe that the total attenuation coefficient α_t of our mixtures can be represented as the following:

$$\alpha_t = \alpha_1 + \alpha_2 + \alpha_3 \qquad \textit{Eq. 1}$$

where α_1 is attenuation coefficient of β-haematin, α_2 is the coefficient blood, and α_3 is the synergistic attenuation coefficient for both together. This ΔOD varies with wavelength, is statistically significant, and likely due to multiple scattering between β-haematin and blood. Multiple scattering arises when a photon travels through a turbid media and it encounters more than one scattering centre. The presence of BH in blood increases the number of scattering centres (Fig. 5A) and thus the amount of multiple scattering.

For blood and β-haematin alone, their attenuation coefficient is the sum of both scattering and absorbing components. Written individually for β-haematin, this is as follows:

$$\alpha_1 = \alpha_{1a} + \alpha_{1s} \qquad \textit{Eq. 2}$$

where α_{1a} is the attenuation component due to absorption and α_{1s} is due to light scattering. For a suspension of BH and blood, this equation is represented as:

$$\alpha_t = \alpha_{1a} + \alpha_{1s} + \alpha_{2a} + \alpha_{2s} + \alpha_3 \qquad \textit{Eq. 3}$$

where α_3 is the coefficient for synergistic attenuation enhancement ΔOD. The presence of α_3 effectively decreases the probability p that an incident photon can have a free path l passing through the media.

$$p(l) = \frac{I_l}{I_0} = e^{-\alpha_t l} \qquad \textit{Eq. 4}$$

where I_l is the intensity at a distance l from the location where the beam enters the medium and I_0 the incident intensity [34]. The light transmission through the sample is:

$$T = \frac{I}{I_0} = e^{-\alpha_t l} \qquad \textit{Eq. 5}$$

where I is equal to I_l. Equations to this point assume that α_s is completely isotropic so that its g, the anisotropy factor, is equal to zero. This is a reasonable assumption because

while individual BH crystals are anisotropic, their net orientation in solution is random in the absence of external forces.

Using our understanding of α_t and our experimental results, we developed a model of our custom reader. Our devices measures the ratio of light intensity on both detectors, expressed as:

$$\frac{I_{545}}{I_{645}} = Ae^{-\alpha_{t(545)}l+\alpha_{t(645)}l} \qquad \text{Eq. 6}$$

where A is the equal to the ratio of the incident intensities, $I_{0(545)}/I_{0(645)}$, which can be determined from the spectra of the LED light source. I_{545} is the intensity at the first detector with a 540-550 nm bandpass filter and the I_{645} is the intensity at the second detector with 640-650 nm bandpass filter. α_t can be estimated for each of the wavelength ranges since the attenuation for blood and BH were measured independently and α can be estimated from the measured ΔODs. The light on each detector is converted into voltage based on the photodiode responsiveness, op amp electronics, and system noise.

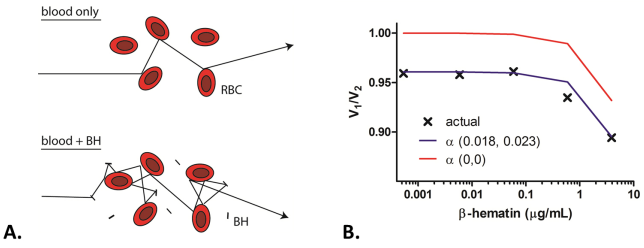

Figure 5. Possible mechanism and model of synergistic attenuation enhancement of BH in blood. (A) Multiple scattering of light in blood in the absence and presence of BH. BH, a highly scattering crystal, increases the amount of multiple scattering in the mixture. (B) Mathematical model of the SAE effect. The red line, α_3 (0, 0), shows the expected result of V_1/V_2 without the SAE effect. The blue line shows the SAE effect utilizing values α_3 (0.018, 0.023). α_3 (645 nm, 545 nm) = α_3 at 645 nm and 545 nm wavelengths, respectively.

In Fig. 5B**,** plots with and without α_3 are compared with the actual data. In the absence of synergistic attenuation enhancement, the voltage ratio V_1/V_2 is asymptotic with 1 as the BH concentration decreases. In the experimental data, V_1/V_2 approaches 0.96. This can be accounted for by incorporating α_3 (645 nm) = 0.018 and α_3 (545 nm) = 0.023. These values and their relative ratios are consistent with the spike-in experiments performed using conventional spectrophometry (Fig. 1B) and also our LED device (Fig. 4H). Both the experiments and the model suggest that once a particular concentration of BH is reached in blood, α_3 accounts for a consistent increase in light attenuation. Once the concentration of BH reaches approximately 5 μg/mL, attenuation due to its measured extinction dominate.

Our observation is consistent with total optical density $OD_{tot} = OD_{scat} + OD_{abs}$, where OD_{scat} is the measure of the coherent and incoherent scattering and OD_{abs} is the absorption [35], which is linear with respect to hematocrit and BH concentration. Our observed ΔOD is a direct contribution from the scattering contribution, which is dependent on photodiode aperture, particle size, particle composition, wavelength, cell refractive index, and plasma refractive index [36,37].

5 Conclusions

Here, we describe data showing the presence of BH in blood leads to synergistic attenuation enhancement. This is observed down to pg/mL concentrations of BH. Based on calculations of the extinction of BH, at least 10^6-fold greater concentrations of BH are required for detection. This enhancement in attenuation is due to synergistic effects with blood. The presence of the SAE effect with BH in blood means that light transmission through a bulk solution can be utilised to detect the presence of malarial BH. The presence of the SAE effect was verified using an LED -based custom scanner, consisting of components typically found in a pulse oximeter. The experimental results agree with a model for SAE.

While work needs to be done on exploring the basis for the SAE effect, the unique scattering characteristics of BH and HZ are likely contributory. These crystals are polydisperse, birefringent, and are between 300–500 nm in length and 50–150 nm in width [38]. For solutions of BH and HZ without blood, the Mie solution to Maxwell's equations can be applied to the observed scattering and to distinguish stages of extracted parasites [17,18,39]. Based on refractive index maps of *Plasmodium falciparum* [20], HZ has a greater index of refraction than erythrocyte contents and its hemoglobin. The optical properties of HZ lead to unique light scattering properties, which have been measured using elastic scattering methods[17] and studied via combined dark-field and cross polarisation imaging [27]. These scattering studies have been largely performed on blood smears, which is different than bulk solutions.

In bulk samples, there are more blood cells, thus more scattering centres, and increasing the odds of multiple scattering. Multiple scattering can increase the effective path length of light travelled through the sample and lead to increased attenuation as observed for both orthogonal directions. Based on Twersky's analytical multiple scattering theory of biological suspensions [37], multiple scattering is based on particle size, wavelength, plasma refractive index, and cell refractive index. In our test system, the BH crystals have different sizes and refractive indices than

blood cells. Whether or not these changes are sufficient to explain the SAE effect remains to be studied. Although BH crystals are scattering centres, there is no net observed increase in light scattering at 90° because it is likely light is absorbed by neighbouring red blood cells, which is based on the absorbance spectra of the blood cells. When compared with the expected detection sensitivity of BH in blood, there is a 10^6-fold enhancement of the attenuation. The magnitude of this effect is dependent on the concentration of blood. The greater the blood concentration, the greater the effect, based on comparison of the mass attenuation coefficient for BH in 1% Hct diluted blood, BH in 50% Hct whole blood, and various analyses of λ ratios. An increasing concentration of blood leads to a greater number of scattering and absorbing centres. Confounding factors to the SAE have been ruled out. This includes oxygenation changes upon hemozoin addition. In the metabolism of hemoglobin to hemozoin, Fe^{2+} is reduced to Fe^{3+}, which cannot bind oxygen [31]. Also, the purity of the BH samples was verified by FTIR (Supplemental data). Complete blood count measurements before and after spike-in show no changes, ruling out platelet aggregation and any other cell-level changes (Supplemental data). In all our time course experiments the SAE effect reaches a maximum after a timescale of minutes. At present, possible explanations include equilibration of the BH with the blood sample, binding of the BH to the cells, internalisation of the BH by cells, or surface adsorption to the cuvette. To rule out localisation of BH in cells, we performed polarised microscopy on mixtures of blood and BH, which yielded no obvious areas of localisation (data not shown). Our BH spike-in experiments and BH titration in 1x PBS rule out the SAE effect arising from surface adsorption of BH to the walls of the cuvette (Fig. 2G-I, Supplemental data).

The high sensitivity of our method likely corresponds to a low parasitemia level. Of the ~ 1.8 fmol of Fe(II)PPIX in a blood cell 25-30% is converted to hemozoin, which corresponds to 0.3 pg HZ/RBC for an estimation of parasitemia [31-33]. At the lowest tested BH concentration of 6 pg/mL, this is 20 infected cells/mL. This corresponds to 0.020 infected cells/μL. We typically utilised 10-fold diluted blood for our experiments so this would correspond to 0.2 infected cells/μL in a whole blood sample. This value is well below the WHO recommended 100 parasites/μL. The estimation of hemozoin per infected RBC varies based on the parasite stage and likely varies between individuals and the progression of the disease. The ring, trophozoite, schizont, and gametocyte stages all contain hemozoin, although in different amounts. This has been explored recently in an article using depolarised side scatter to quantify the amount of hemozoin in peripheral blood of infected individuals versus cell culture [40]. For instance, the pigmented trophozoite stage has a higher hemozoin concentration than the ring stage. This paper raised the concern that most circulating intra-erythrocytic *P. falciparum* contain little or no hemozoin. The trophozoites and schizonts, however, can remain bound to endothelial cells in the circulatory system to account for the differences between malaria culture and extracted blood from infected patients. Free hemozoin has also been measured in plasma; for instance, high plasma hemozoin has been shown to suppress erythropoiesis [41]. The total hemozoin concentration is thus the sum of the content inside infected peripheral blood cells, infected sequestered blood cells, and plasma hemozoin, which requires further study. A non-invasive detection method would interrogate all hemozoin in the tissue, regardless of sequestration, and thus would offer advantages over methods that require interrogation of hemozoin in blood obtained by fingerstick or venipuncture [42-48].

The findings here are consistent with a minimally invasive diagnostic method. One approach for minimal invasive diagnosis is ratiometric wavelength analysis of trace amounts hemozoin in a small drop of blood although this would be subject to sequestration issues previously discussed. Another approach is non-invasive detection. For this, there are several considerations. The scattering from tissues may have additional effects on SAE. Light penetration through the skin also needs to be considered. The wavelengths 645, 805, or 940 nm are similar to those utilised in pulse oximetry. The 540–550 nm range requires a shorter path length, such as the tip of the finger or earlobe. The effects of melanin are unlikely to impact the device since it is not strongly absorbing at our wavelengths. The addition of tissue, integument, blood vessels, and bone adds additional baseline attenuation to the signal such that:

$$\alpha_t = \alpha_1 + \alpha_2 + \alpha_3 + \alpha_4 \qquad \textit{Eq. 7}$$

where α_1 is the attenuation coefficient of BH, α_2 is the coefficient of blood, α_3 is the SAE coefficient, and α_4 is the tissue coefficient. In our experiments, we observed the SAE effect with and without frosted glass windows on the cuvette. The frosted glass is an analog for α_4. While this is the case work needs to be performed on actual tissue. Based on analogous spectral [26] and structural studies [12] of β-haematin to hemozoin, our experiments presented are directly applicable to the detection of hemozoin released extracellularly with ruptured schizonts in the erythrocytic cycles. Additional work is needed to study the optical effects of intracellular hemozoin. Different species of *Plasmodium* have demonstrated differences in hemozoin morphology [38], which may lead to different ΔOD changes. *Plasmodium* is not the only organism that synthesizes hemozoin. For instance, *Schistosoma mansoni* synthesises a similar heme polymer [49]. A diagnostic approach using SAE needs to be performed in context of the potential sources of hemozoin and the overall clinical pic-

ture. In order for a minimally-invasive device to be practical, it also needs to account for blood oxygenation, which can be confounded by conditions such as methemoglobinemia [50]. For cost-effectiveness, the device needs to utilise mass produced components, such as photodiodes and LEDs.

6 Future Perspectives

The next steps in our research include building and testing a LED scanner on *Plasmodium* infected samples and tissue -based samples. Multiple areas need to be addressed including further work on the mechanism of the SAE effect and implementation in actual clinical settings. Our GCE grant catalysed this new effort and research area.

7 Acknowledgement

This work was funded by the Bill & Melinda Gates Foundation Grand Challenges Exploration grant OPP1017986.

References

1. See: www.who.int/topics/malaria/en/
2. Milne LM, Kyi MS, Chiodini PL, Warhurst DC: Accuracy of routine laboratory diagnosis of malaria in the United Kingdom. *J. Clin. Pathol.* 1994, **47**:740-742.
3. Wongsrichanalai C, Barcus MJ, Muth S, Sutamihardja A *et al.*: A review of malaria diagnostic tools: microscopy and rapid diagnostic test (RDT). *Am. J. Trop. Med. Hyg.* 2007, **77**:119-127.
4. Moody AH, Chiodini PL: Non-microscopic method for malaria diagnosis using OptiMAL IT, a second-generation dipstick for malaria pLDH antigen detection. *Br. J. Biomed. Sci.* 2002, **59**:228-231.
5. Saiki RK, Gelfand DH, Stoffel S, Scharf SJ *et al.*: Primer-directed enzymatic amplification of DNA with a thermostable DNA polymerase. *Science* 1988, **239**:487-491.
6. Long GW, Jones TR, Rickman LS, Trimmer R *et al.*: Acridine orange detection of *Plasmodium falciparum* malaria: relationship between sensitivity and optical configuration. *Am. J. Trop. Med. Hyg.* 1991, **44**:402-405.
7. Hanscheid T, Frita R, Langin M, Kremsner PG *et al.*: Is flow cytometry better in counting malaria pigment-containing leukocytes compared to microscopy? *Malar. J.* 2009, **8**:255.
8. Frita R, Rebelo M, Pamplona A, Vigario AM *et al.*: Simple flow cytometric detection of haemozoin containing leukocytes and erythrocytes for research on diagnosis, immunology and drug sensitivity testing. *Malar. J.* 2011, **10**:74.
9. Adams PA, Egan TJ, Ross DC, Silver J, *et al.*: The chemical mechanism of beta-haematin formation studied by Mossbauer spectroscopy. *Biochem. J.* 1996, **318(Pt 1)**:25-27.
10. Slater AF, Swiggard WJ, Orton BR, Flitter WD *et al.*: An iron-carboxylate bond links the heme units of malaria pigment. *Proc. Nat. Acad. Sci. USA* 1991, **88**:325-329.
11. Bohle DS, Dinnebier RE, Madsen SK, Stephens PW: Characterization of the products of the heme detoxification pathway in malarial late trophozoites by X-ray diffraction. *J. Biol. Chem.* 1997, **272**:713-716.
12. Pagola S, Stephens PW, Bohle DS, Kosar AD *et al.*: The structure of malaria pigment beta-haematin. *Nature* 2000, **404**:307-310.
13. Serebrennikova YM, Patel J, Garcia-Rubio LH: Interpretation of the ultraviolet-visible spectra of malaria parasite Plasmodium falciparum. *Appl. Opt.* 2010, **49**:180-188.
14. Orjih AU, Fitch CD: Hemozoin production by Plasmodium falciparum: variation with strain and exposure to chloroquine. *Biochim. Biophys. Acta* 1993, **1157**:270-274.
15. Lawrence C, Olson JA: Birefringent hemozoin identifies malaria. *Am. J. Clin. Pathol.* 1986, **86**:360-363.
16. Wilson BK, Behrend MR, Horning MP, Hegg MC: Detection of malarial byproduct hemozoin utilizing its unique scattering properties. *Opt. Express* 2011, **19**:12190-12196.
17. Lee S, Lu W: Using elastic light scattering of red blood cells to detect infection of malaria parasite. *IEEE transactions on bio-medical engineering* 2012.
18. Park Y, Diez-Silva M, Fu D, Popescu G *et al.*: Static and dynamic light scattering of healthy and malaria-parasite invaded red blood cells. *J. Biomed. Opt.* 2010, **15**:020506.
19. Park Y, Diez-Silva M, Popescu G, Lykotrafitis G *et al.*: Refractive index maps and membrane dynamics of human red blood cells parasitized by Plasmodium falciparum. *Proc. Nat. Acad. Sci. USA* 2008, **105**:13730-13735.
20. Newman DM, Heptinstall J, Matelon RJ, Savage L *et al.*: A magneto-optic route toward the in vivo diagnosis of malaria: preliminary results and preclinical trial data. *Biophys. J.* 2008, **95**:994-1000.
21. Wang C, Trofimov I, Lewis I: Non-Invasive Malaria Detection Using Infrared Spectroscopy. In: *2011 Summer Workshop, Mirthe Center 2011; Princeton, NJ*; 2011.
22. Mens PF, Matelon RJ, Nour BYM, Newman DM *et al.*: Laboratory evaluation on the sensitivity and specificity of a novel and rapid detection method for malaria diagnosis based on magneto-optical technology (MOT). *Malar. J.* 2010, **9**:207.
23. Kramer K, Elam JO, Saxton GA, Elam WN, Jr.: Influence of oxygen saturation, erythrocyte concentration and optical depth upon the red and near-infrared light transmittance of whole blood. *Am. J. Physiol.* 1951, **165**(1):229-246.
24. Loewinger E, Gordon A, Weinreb A, Gross J: Analysis of a micromethod for transmission oximetry of whole blood. *J. Appl. Physiol.* 1964, **19**:1179-1184.
25. Webster JG: Design of Pulse Oximeters. Bristol, UK: Institute of Physics Publishing; 1997.
26. Orjih AU: On the mechanism of hemozoin production in malaria parasites: activated erythrocyte membranes promote beta-hematin synthesis. *Exp. Biol. Med. (Maywood)* 2001, **226**:746-752.
27. Wilson BK, Behrend MR, Horning MP, Hegg MC: Detection of malarial byproduct hemozoin utilizing its unique scattering properties. *Opt. Express* 2011, **19**:12190-12196.
28. Lee S, Lu W: Using elastic light scattering of red blood cells to detect infection of malaria parasite. *IEEE Trans. Biomed. Eng.* 2011, **59**:150-155.

29. Pasternack RF, Goldsmith JI, Szep S, Gibbs EJ: A spectroscopic and thermodynamic study of porphyrin/DNA supramolecular assemblies. *Biophys. J.* 1998, **75**:1024-1031.
30. Pasternack RF, Collings PJ: Resonance light scattering: a new technique for studying chromophore aggregation. *Science* 1995, **269**:935-939.
31. Sullivan DJ, Jr.: Hemozoin: a biocrystal synthesized during the degradation of hemoglobin. In: *Miscellaneous Biopolymers, Biodegradation of Synthetic Polymers.* (Matsumura S, Steinbuchel A, Eds.) Wiley-VCH Verlag GmbH & Co, 2002: 129-163.
32. Ginsburg H, Famin O, Zhang J, Krugliak M: Inhibition of glutathione-dependent degradation of heme by chloroquine and amodiaquine as a possible basis for their antimalarial mode of action. *Biochem. Pharmacol.* 1998, **56**:1305-1313.
33. Ginsburg H, Ward SA, Bray PG: An integrated model of chloroquine action. *Parasitol. Today* 1999, **15**:357-360.
34. Graaff R, Koelink MH, de Mul FF, Zijistra WG *et al.*: Condensed Monte Carlo simulations for the description of light transport. *Appl. Opt.* 1993, **32**:426-434.
35. Steinke JM, Shepherd AP: Role of light scattering in whole blood oximetry. *IEEE Trans. Biomed. Eng.* 1986, **33**:294-301.
36. de Kock JP, Tarassenko L: Pulse oximetry: theoretical and experimental models. *Med. Biol. Eng. Comput.* 1993, **31**:291-300.
37. Twersky V: Absorption and multiple scattering by biological suspensions. *J. Opt. Soc. Am.* 1970, **60**:1084-1093.
38. Noland GS, Briones N, Sullivan DJ, Jr.: The shape and size of hemozoin crystals distinguishes diverse Plasmodium species. *Mol. Biochem. Parasitol.* 2003, **130**:91-99.
39. Serebrennikova YM, Patel J, Garcia-Rubio LH: Interpretation of the ultraviolet-visible spectra of malaria parasite Plasmodium falciparum. *Appl. Opt.* 2010, **49**:180-188.
40. Rebelo M, Shapiro HM, Amaral T, Melo-Cristino J *et al.*: Haemozoin detection in infected erythrocytes for Plasmodium falciparum malaria diagnosis-prospects and limitations. *Acta Trop.* 2012, **123**:58-61.
41. Casals-Pascual C, Kai O, Cheung JO, Williams S *et al*: Suppression of erythropoiesis in malarial anemia is associated with hemozoin in vitro and in vivo. *Blood* 2006, **108**:2569-2577.
42. Samson EB, Goldschmidt BS, Whiteside PJ, Sudduth AS *et al.*: Photoacoustic spectroscopy of beta-hematin. *J. Opt.* 2012, **14**:065302.
43. Mens PF, Matelon RJ, Nour BY, Newman DM *et al.*: Laboratory evaluation on the sensitivity and specificity of a novel and rapid detection method for malaria diagnosis based on magneto-optical technology (MOT). *Malar. J.* 2010, **9**:207.
44. Nyunt M, Pisciotta J, Feldman AB, Thuma P *et al.*: Detection of Plasmodium falciparum in pregnancy by laser desorption mass spectrometry. *Am. J. Trop. Med. Hyg.* 2005, **73**:485-490.
45. Karl S, Gutierrez L, House MJ, Davis TM *et al.*: Nuclear magnetic resonance: a tool for malaria diagnosis? *Am. J. Trop. Med. Hyg.* 2011, **85**:815-817.
46. Belisle JM, Costantino S, Leimanis ML, Bellemare MJ *et al.*: Sensitive detection of malaria infection by third harmonic generation imaging. *Biophys. J.* 2008, **94**:L26-28.
47. Zoueu JT, Zan SG: Trophozoite stage infected erythrocyte contents analysis by use of spectral imaging LED microscope. *J. Microsc.* 2012, **245**:90-99.
48. Yuen C, Liu Q: Magnetic field enriched surface enhanced resonance Raman spectroscopy for early malaria diagnosis. *J. Biomed. Opt.* 2012, **17**:017005.
49. Chen MM, Shi L, Sullivan DJ, Jr.: Haemoproteus and Schistosoma synthesize heme polymers similar to Plasmodium hemozoin and beta-hematin. *Mol. Biochem. Parasitol.* 2001, **113**:1-8.
50. Barker SJ, Tremper KK, Hyatt J: Effects of methemoglobinemia on pulse oximetry and mixed venous oximetry. *Anesthesiology* 1989, **70**:112-117.
51. Blauer G, Akkawi M: Investigations of B- and beta-hematin. *J. Inorg. Biochem.* 1997, **66**:145-152.
52. Blauer G, Akkawi M: B-hematin. *Biochem. Mol. Biol. Int.* 1995, **35**:231-235.
53. Martiney JA, Cerami A, Slater AF: Inhibition of hemozoin formation in Plasmodium falciparum trophozoite extracts by heme analogs: possible implication in the resistance to malaria conferred by the beta-thalassemia trait. *Mol. Med.* 1996, **2**:236-246.
54. Northam L, Baranoski GV: A novel first principles approach for the estimation of the sieve factor of blood samples. *Opt. Express* 2010, **18**:7456-7469.
55. Finlay JC, Foster TH: Effect of pigment packaging on diffuse reflectance spectroscopy of samples containing red blood cells. *Opt. Lett.* 2004, **29**:965-967.

Annex: Materials and Methods

β-haematin synthesis: We utilised a protocol previously described in the literature [51-53]. The β-haematin was synthesised by a contract chemical synthesis company (AsisChem, IN). In brief, a solution of haemin (0.2 g, 0.31 mmol) was heated to 37°C in 0.4M NaOH aqueous (12.6 mL) and water (11.2 mL). Glacial acetic acid was added drop-wise (12.2 mL) and the resulting solution was stirred at 37°C for 2 hours. The reaction mixture was allowed to cool to room temperature and the resulting precipitate was washed exhaustively with distilled water, DMSO, and ethanol. The material was dried to give 150 mg of β-haematin. The product was confirmed by FTIR for a characteristic 1662.5 cm^{-1} peak. The absorbance spectra of β-haematin was measured at 50 µg/mL in 1x phosphate buffered saline (PBS) using a Spectramax M2 (Molecular Devices, CA).

Spectroscopy: All spectroscopic measurements were performed with a commercial combination cuvette and microplate reader (SpectraMax M2, Molecular Devices, CA). The device was warmed up for at least 15 minutes prior to each use. Quartz cuvettes (Starna, CA) with path

lengths of 10 mm and 4 mm were utilised. Various combinations of frosted and clear cuvettes were utilised. The cuvettes were rinsed with 1x PBS and air-dried prior to use. Special care was taken to ensure that all glass surfaces were clean prior to measurements. This was done by rinsing the inside and outside of the cuvettes with ethanol followed by three dH_2O washes. The cuvettes were air-dried prior to use. Spike-in and titration experiments were performed to ensure that measurements were taken with the same cuvette in an identical orientation. The absolute optical densities (OD) of the measurements were recorded using Softmax Pro software (Molecular Devices, CA). Anonymous human blood samples with K_2EDTA as an anticoagulant were purchased from Innovative Research (Novi, MI). Blood was equilibrated to room air and temperature for an hour prior to the experiments. Blood dilutions were performed with 1x PBS with 5.5 mM K_2EDTA. For the time course experiments, data points were taken at timed intervals, in sets of three data points. For each spike-in, the sample was mixed with a 1 mL pipette up and down to avoid incorporation of any air bubbles. The BH samples utilised were either synthesised or purchased (Invivogen, CA). BH stock concentrations were made by sonicating 1 mg of crystal in 1 mL of 1x PBS for 8 hours at 37°C. The result was a dark suspension of BH crystals. Samples were vortexed vigorously prior to use. Sample titrations were obtained from these stock solutions. *p*-Values for the experiments were performed with GraphPad Prism (GraphPad Software, CA) using an unpaired *t*-test. Data was plotted with GraphPad Prism or MS Excel.

Light scattering experiments: 90° scattering experiments were performed using the SpectraMax M2 by setting the excitation wavelength equal to the emission wavelength and using the photomultiplier tube orthogonal to the excitation source. The cuvette was taped off using black photographic tape (3M, MN) to prevent detector saturation and also effect of bubbles near the top of the cuvette. A small, square-shaped hole was cut in the tape and utilised as the aperture for the excitation source. The centre of the hole was 0.65 inches from the bottom of the cuvette to match the location of the excitation source. A similar exit aperture was placed in front of the PMT to prevent detector saturation. Data was acquired at defined time intervals, in sets of three data points. Blood and BH samples are identical to the attenuation experiments. Samples were periodically mixed by pipetting up and down to prevent settling. The BH spike-in was performed in an identical manner to the attenuation experiments. Triplicate measurements were performed for each data point. Data collection was done with Softmax Pro and analysed with GraphPad Prism and MS Excel.

LED scanner custom apparatus: The main body of the optical finger scanner hardware comprises a 6000 mcd 3 mm white LED with a 20 degree viewing angle (FCB Electronics, MI), two PDB-C609-2 large area blue enhanced silicon photodiodes (Advanced Photonix, MI), a 540-550 nm bandpass 3rd Millennium filter (Omega Filters, VT), a 640-650 nm bandpass 3rd Millennium filter, and a self-masking semi-micro blackened cuvette (Starna, CA). The optomechanical enclosure was printed in a photoplastic using a VFlash 3D modeler (3D Systems, SC). The output from each photodiode is connected to an input terminal of an AD620 instrumentation op amp for differential amplification. The first amplification stage has 50.4x gain. The output from the first op amp is amplified by a second AD620 for a total of greater than 10^5 signal amplification. The instrumentation op amps are powered by two 9V batteries in series, with the 9V connection point serving as the virtual ground. The LED is separately powered by two AAA batteries. The LED is digitally controlled by a transistor and its intensity adjusted by a 100Ω CT6ER101 trimmer. The amplified voltage output is converted to a digital signal by a NI-6008 USB 2.0 data acquisition (DAQ) card (National Instruments, TX) connected to a Toshiba Portege R835 with an Intel Core i3 processor running LabVIEW 2009 Professional. Custom LabVIEW software was utilised to collect and save the data. For data analysis, digital filtering with a low pass filter at 1 Hz was utilised to remove high frequency noise. Data was averaged over 1 second for each condition.

LED scanner spike-in experiments: The synthesised β-haematin, in powder form, was resuspended in 1x PBS to a final concentration of 1 mg/mL. The suspension was sonicated at 37°C for 8 hrs until there were no visible particulates. BH was serially diluted 10-fold for the various titration points. Anonymous whole human blood samples (Innovative Research, MI) were obtained for testing in K_2EDTA BD Vacutainer tubes. 1.5 mL of 4% Hct human blood (v/v) in 1x PBS was pipetted into identical self-masking blackened semi-micro cuvettes with 1 cm path lengths (Starna, CA). The lower blood concentration was utilised to approximate the transmission of light through a finger. To control for any cuvette or insertion differences, two blank samples with blood only were measured sequentially and the voltage level recorded. Increasing concentrations of β-haematin was spiked into one of the cuvettes and the measurement protocol repeated. Special care was taken to avoid blood settling in the tube by inverting the tubes frequently. Stray light was avoided by performing the experiments in the dark and blocking any sources of light.

Data analysis for LED scanner experiments: A custom LabVIEW programme was utilised to analyse the raw data. Data over 1s was averaged to obtain a voltage meas-

urement for each cuvette reading. For measurements at a given concentration, the voltage difference between the β-haematin and the blood only samples were recorded. The mean, standard deviation (SD), and standard error of the mean (SEM) of these voltage differences were tabulated. The *p*-values of the measurements were determined using an unpaired two-tailed t-test between the blanks and the spike-in titrations. The level of estimated parasitemia was determined from the ratio of β-haematin to blood cells. This approach ensured a fixed amount of BH per red blood cell (RBC) for parasitemia calculations. Error propagation performed using conventionally accepted techniques and statistics were performed with GraphPad (GraphPad Software, CA) and MS Excel.

Competing interests: No competing interests declared.